

Published in final edited form as:

*Cell Signal.* 2012 December ; 24(12): 2349–2359. doi:10.1016/j.cellsig.2012.08.011.

## The Gβ3 splice variant associated with the C825T gene polymorphism is an unstable and functionally inactive protein

Zhizeng Sun<sup>1</sup>, Caitlin Runne<sup>1</sup>, Xiaoyun Tang<sup>1</sup>, Fang Lin<sup>2</sup>, and Songhai Chen<sup>1,3,4</sup>

<sup>1</sup>Department of Pharmacology, University of Iowa, Iowa City, Iowa, USA 52242

<sup>2</sup>Departments of Anatomy and Cell Biology, University of Iowa, Iowa City, Iowa, USA 52242

<sup>3</sup>Department of Internal Medicine, Roy J. and Lucille A. Carver College of Medicine, University of Iowa, Iowa City, Iowa, USA 52242

### Abstract

A splice variant of G<sub>β3</sub>, termed G<sub>β3s</sub>, has been associated with the C825T polymorphism in the G<sub>β3</sub> gene and linked with many human disorders. However, the biochemical properties and functionality of G<sub>β3s</sub> remain controversial. Here, using multidisciplinary approaches including co-immunoprecipitation analysis and bioluminescence resonance energy transfer (BRET) measurements, we showed that unlike G<sub>β3</sub>, G<sub>β3s</sub> failed to form complexes with either G<sub>α</sub> or G<sub>γ</sub> subunits. Moreover, using a mutant G<sub>α2</sub> deficient in lipid modification to purify G<sub>β3s</sub> from Sf9 cells without the use of detergents, we further showed that the failure of G<sub>β3s</sub> to form dimers with G<sub>α</sub> was not due to the instability of the dimers in detergents, but rather, reflected the intrinsic properties of G<sub>β3s</sub>. Additional studies indicated that G<sub>β3s</sub> is unstable, and unable to localize properly to the plasma membrane and to activate diverse G<sub>α</sub> effectors including PLC<sub>2/3</sub>, PI3K, ERKs and the Rho guanine exchange factor (RhoGEF) PLEKHG2. Thus, these data suggest that the pathological effects of G<sub>β3</sub> C825T polymorphism may result from the downregulation of G<sub>β3</sub> function. However, we found that the chemokine SDF1 transmits signals primarily through G<sub>α1</sub> and G<sub>α2</sub>, but not G<sub>α3</sub>, to regulate chemotaxis of several human lymphocytic cell lines, indicating the effects of G<sub>β3</sub> C825T polymorphism are likely to be tissue and/or stimuli specific and its association with various disorders in different tissues should be interpreted with great caution.

### Keywords

Heterotrimeric G protein; GPCR; GNB3; signalling; polymorphism; chemotaxis

### 1. Introduction

G protein coupled receptors (GPCRs) are the largest family of cell surface receptors and play a critical role in many physiological processes, including neurotransmission, metabolism, cardiovascular regulation and leukocyte migration [1, 2]. Dysregulation of GPCRs has been associated with many diseases, including hypertension, obesity, diabetes and tumorigenesis [3-8].

<sup>4</sup>Address correspondence to: Songhai Chen, M.D., Ph.D., Bowen Science Building, Room 2-452, 51 Newton Road, Iowa City, IA 52242. Tel: 319-384-4562; Fax: 319-335-8930; songhai-chen@uiowa.edu.

**Publisher's Disclaimer:** This is a PDF file of an unedited manuscript that has been accepted for publication. As a service to our customers we are providing this early version of the manuscript. The manuscript will undergo copyediting, typesetting, and review of the resulting proof before it is published in its final citable form. Please note that during the production process errors may be discovered which could affect the content, and all legal disclaimers that apply to the journal pertain.

GPCRs transmit extracellular signals through the heterotrimeric G protein, which is composed of the G $\alpha$  subunit and the obligate G $\beta\gamma$  dimer. Multiple isoforms of each subunit have been identified, including twenty-three G $\alpha$ , six G $\beta$ , and thirteen G $\gamma$  subunits [1, 2]. These different subunits can pair to form heterotrimeric G proteins with unique compositions that may define their specificity and selectivity in coupling to receptors and activation of downstream effectors [9]. Activation of G proteins is initiated by receptor-catalyzed exchange of GDP for GTP on G $\alpha$  subunits, and the dissociation of G $\beta\gamma$  from G $\alpha$  subunits. Both the activated G $\alpha$  and G $\beta\gamma$  subunits can stimulate distinct downstream signaling cascades through diverse effectors, including phospholipases, kinases, ion channels and interacting proteins [1].

Six well characterized G $\alpha$  isoforms are encoded by five distinct genes, G $\alpha_1$ , G $\alpha_2$ , G $\alpha_3$ , G $\alpha_4$  and G $\alpha_5$  [9]. Alternate splicing of the G $\alpha_5$  gene generates two G $\alpha_5$  isoforms, the long and short G $\alpha_5$ . Additionally, a number of genetic polymorphisms in G $\alpha_3$  have been identified and are associated with the occurrence of various shorter G $\alpha_3$  splice variants [10-13]. One of the best characterized G $\alpha_3$  polymorphisms is a C825T polymorphism, which is associated with an alternative splicing of exon 9 in the G $\alpha_3$  gene, resulting in an in-frame deletion of 123-bp that encodes a WD40-repeat domain in G $\alpha_3$  [10]. The resultant G $\alpha_3$  splice variant is 41 amino acids shorter than the wild-type G $\alpha_3$  and is termed G $\alpha_3s$ . The G $\alpha_3$  C825T polymorphism was originally identified in cultured lymphocytes from patients with essential hypertension and enhanced Na<sup>+</sup>/H<sup>+</sup> exchange activity [10]. Subsequent studies found that the C825T allele occurs most frequently in Black Africans (79%), followed by Mongoloids (46%) and Caucasians (36%) [14]. In population-based association studies, the G $\alpha_3$  C825T polymorphism has been associated with an increased risk for diverse disorders, including hypertension, obesity, diabetes, depression, and tumorigenesis [15-17]. It may also serve as a pharmacogenetic marker to predict treatment responses for various diseases [14]. Nevertheless, conflicting data regarding the association of C825T polymorphism with various disorders have also been reported [18-22].

Despite the lack of one WD40 domain, initial studies from Siffert's group showed that G $\alpha_3s$  can still form dimers with various G $\beta\gamma$  subunits in heterologous expression systems [23]. Moreover, as compared to the wild-type G $\alpha_3$ , G $\alpha_3s$  was found to display enhanced ability to mediate GPCR-stimulated GTP/GDP exchange on G $\alpha_i$  subunits and to stimulate a G $\alpha_i$  effector, ERKs [13]. Based on these findings, it has been speculated that many disorders associated with the G $\alpha_3$  C825T polymorphism are mediated by the gain-of-function of G $\alpha_3s$  signaling. However, in contrast to these findings, Ruiz-Velasco et al. reported that, when overexpressed in rat sympathetic neurons, G $\alpha_3s$  failed to either form a complex with G $\alpha_2$  or G $\alpha_{i2}$ , or modulate N-type Ca<sup>2+</sup> and G protein-gated inwardly rectifying K<sup>+</sup> channels [24]. Using a rabbit reticulocyte lysate expression system *in vitro*, Dingus et al. also reported that unlike G $\alpha_3$ , G $\alpha_3s$  did not form dimers with various G $\beta\gamma$  subunits [25]. Nevertheless, whether G $\alpha_3s$  can form complexes with G $\beta\gamma$  subunits and stimulate many other G $\alpha_i$  effector in cells has not been systematically evaluated. Moreover, the function of G $\alpha_3$  and G $\alpha_3s$  has not been established in cells/tissues endogenously expressing these proteins. Thus, despite the fact that the physiological and pathological implications of G $\alpha_3s$  have been extensively studied, the biochemical properties and functionality of G $\alpha_3s$  remains uncertain. This may in part account for the current confusion about the significance of G $\alpha_3$  C825T allele in multiple disorders.

In this study, we used multiple approaches to systematically assess the ability of G $\alpha_3s$  to function as a canonical G $\alpha$  protein. We show here that G $\alpha_3s$  was deficient in interaction with either G $\beta$  or G $\gamma$  in various expression systems, using multi-disciplinary approaches including co-immunoprecipitation and bioluminescence resonance energy transfer (BRET) assays. We further show that G $\alpha_3s$  failed to couple to GPCRs and to stimulate diverse G

effectors including PLC, PI3K, ERKs and RhoGEFs. Moreover, as compared to G<sub>3</sub>, G<sub>3s</sub> was less stable and did not localize properly to the plasma membrane. Accordingly, although the G<sub>3s</sub> transcript can be identified in several human lymphocytic cell lines containing the C825T allele, these cells did not express detectable G<sub>3s</sub> protein. Intriguingly, we found that SDF1-stimulated signaling and chemotaxis of these cells were not affected by downregulation of G<sub>3</sub>/G<sub>3s</sub> but abolished by inhibition of G<sub>1</sub> and G<sub>2</sub>, suggesting that the function of G<sub>3</sub> and G<sub>3s</sub> is stimuli and/or cell type dependent. Together, our findings demonstrate that G<sub>3s</sub> is an unstable and functionally inactive protein. Therefore, it is likely that the pathological effects of G<sub>3</sub> C825T polymorphism result from a functional downregulation of G<sub>3</sub> activity. Nevertheless, our data indicate that the function of G<sub>3</sub> is stimuli and/or tissue specific. Thus, great caution should be exerted when interpreting the functional consequence of G<sub>3</sub> C825T polymorphism in different tissues.

## 2. Material and methods

### 2.1. Reagents

Mouse anti-FLAG (M2) antibody was from Sigma-Aldrich. Rat anti-HA antibody was from Roche Applied Science (Indianapolis, Indiana, USA). Rabbit anti-G<sub>i1</sub>, anti-G<sub>i2</sub> and anti-G<sub>12</sub> (T20) antibodies were from Santa Cruz Biotechnology (Santa Cruz). Rabbit anti-G<sub>q/11</sub> antibody was from EMD Millipore. Mouse anti-G<sub>s</sub> and anti-His antibodies were from UC Davis/NIH NeuroMab Facility. AKT, phospho-AKT, ERK1/2, and phospho-ERK1/2 antibodies were from Cell Signaling Technology, Inc. Human SDF-1 was from PeproTech. Fura-2/AM, Alexa 488- and Alexa 568-conjugated secondary antibodies and Dynabeads protein G were from Life Technologies. Nickel-nitrilotriacetic acid-agarose (Ni-NTA) beads were from Qiagen. siRNAs against G<sub>1</sub>, G<sub>2</sub> and G<sub>1/2</sub> were from Thermo Fisher Scientific Dharmacon. A siRNA against G<sub>3</sub> was from Life Technologies. All other materials were obtained with highest quality available.

### 2.2. Cell Culture

HEK293 cells and COS-7 cells were obtained from ATCC and grown at 37°C, 5% CO<sub>2</sub> in DMEM (Life Technologies) containing 10% fetal bovine serum (FBS). Jurkat T cells were maintained in RPMI (Life Technologies) supplemented with 10% FBS. B lymphocytic cell lines GM19116C and GM18500B were from Coriell Cell Repositories and maintained in RPMI supplemented with 10% FBS. Sf9 insect cells were grown at 28 °C in Sf900 II serum-free medium (Life Technologies).

### 2.3. Plasmid and Viral Constructs

FLAG-tagged or untagged human G<sub>3</sub>, G<sub>3s</sub>, G<sub>2</sub>, G<sub>5</sub>, G<sub>8</sub>, G<sub>10</sub> and G<sub>12</sub> in pcDNA3.1 were obtained from Missouri S&T cDNA Resource Center. For the bioluminescence resonance energy transfer (BRET) assay the cDNAs encoding G<sub>3</sub> and G<sub>3s</sub> were cloned into pRluc-C (PerkinElmer), while the cDNAs encoding various G subunits were cloned into pGFP<sup>2</sup>-C (PerkinElmer). Baculoviruses encoding FLAG-tagged G<sub>3</sub> and G<sub>3s</sub>, and 6 × His-tagged G<sub>2</sub> and G<sub>5</sub> were generated using the Gateway cloning and the Bac-To-Bac baculovirus expression systems (Life Technologies) as described. Lentiviruses encoding FLAG-tagged G<sub>3</sub> and G<sub>3s</sub> were generated by cloning FLAG-tagged G<sub>3</sub> and G<sub>3s</sub> into the destination vector pLenti-PGK-Puro-DEST vector (Addgene) by the Gateway cloning system and packaged in HEK293FT cells as described [26].

### 2.4. Transfection

Transient transfection of HEK293 cells was performed using PolyJet DNA *in vitro* transfection reagent (Signagen). Stable expression of FLAG-tagged G<sub>3</sub> or G<sub>3s</sub> in HEK293

cells was performed by transducing cells with lentiviruses encoding FLAG-tagged G 3 or G 3s and selecting with 2-20  $\mu\text{g/ml}$  puromycin for about 2 weeks. The puromycin-resistant cells were pooled and maintained in the medium containing 10  $\mu\text{g/ml}$  puromycin.

Transient transfection of COS-7 was performed by using Lipofectamine 2000 or the Neon transfection system (Life Technologies) according to the manufacturer's protocol. Transient transfection of Jurkat T cells with siRNAs (2 nmol/100  $\mu\text{l}$ ) against G 1 (5'-ggataacatttgcctcatttt-3'), G 2 (5'-actgggtacctgtcgtgtttt-3'), a common sequence of G 1 and G 2 (5'-tagcagcactcaactgcatt-3') or G 3 (5'-tcgcaagatgggaagctgatcgtgt-3') was performed by using the Neon transfection system as described previously [26].

#### 2.4. Immunoprecipitation

The interaction of G 3 or G 3s with various G subunits was determined using co-immunoprecipitation assays in HEK293 cells co-transfected with FLAG-tagged G 3 or G 3s and HA-tagged G subunits. Two days post-transfection, cells were lysed in lysis buffer (50 mM Tris-HCl, pH 7.4, 150 mM NaCl, 1 mM EDTA, 1% Nonidet P-40) containing protease inhibitors. HA-G was then immunoprecipitated by protein G Dyna beads pre-coupled with the rat anti-HA antibody. Protein complexes were resolved by SDS-PAGE and analyzed by Western blot analyses. To determine the interaction of G 3 or G 3s with endogenous G , immunoprecipitation was performed in cell lysates prepared from HEK293 cells transfected with FLAG tagged G 3 or G 3s and G 2, using an anti-FLAG antibody.

#### 2.5. Analysis of G $\beta$ /G $\gamma$ Interactions in Sf9 Cells

Subconfluent Sf9 insect cells were infected with baculoviruses encoding FLAG-G 3 or -G 3s and 6  $\times$  His-G 2, -G 5 or G 2C68S. Two days post-infection, cell lysates were prepared using HEPES buffer (20 mM HEPES, pH 8.0, 200 mM NaCl, 10 mM Imidazole, pH 8.0, 0.5% Thesit, 5 mM  $\beta$ -mercaptoethanol) containing protease inhibitors, and were incubated with Ni-NTA beads for 2 hours at 4°C. Protein complexes were washed three times with the HEPES buffer containing 500 mM NaCl, and then resolved by SDS-PAGE and analyzed by Western blotting.

#### 2.6. BRET Assays

HEK293 cells were co-transfected with 100 ng pRluc-G 3 or -G 3s and different amount of pGFP<sup>2</sup>-G subunits in 12-well plates. 48 hr post-transfection, cells were trypsinized and resuspended in Hank's balanced salt solution containing magnesium and calcium (Life Technologies) and 0.1% glucose. Cells ( $1 \times 10^5$ ) were distributed in triplicate into opaque 96-well plates. Subsequently, the luciferase substrate coelenterazine 400a (5  $\mu\text{M}$  final concentration) was added, and luminescence and fluorescence were measured at  $410 \pm 80$  nm and  $515 \pm 30$  nm with the Biotek Synergy 4 microplate reader [27, 28]. BRET signals were determined by calculating the 510/410 nm ratio of light intensity. Net BRET values were determined by subtracting the background signal detected from expression of the pRluc-tagged construct alone.

#### 2.7. Immunofluorescence Staining

The cellular localization of FLAG-G 3 and FLAG-G 3s was determined in HEK293 cells stably expressing these proteins. Cells were fixed with 4% paraformaldehyde and permeabilized with 0.5% Triton-100 for 5 min. Cells were then stained with mouse anti-FLAG (1:500) and rabbit anti-G (T20; 1:800) at room temperature for 1 hr, followed by incubation with the secondary antibodies Alexa 488- and Alexa 568-conjugated anti-mouse and anti-rabbit IgG, respectively. Images were acquired with a LSM510 Meta inverted

confocal microscope (Carl Zeiss) with an argon/krypton laser and a Plan Apo 40× 1.3 NA oil immersion lens, and processed with Adobe Photoshop [26].

## 2.8. Analysis of Gβ3 and Gβ3s Stability

HEK293 cells stably expressing FLAG-G<sub>3</sub> and FLAG-G<sub>3s</sub> were treated with cycloheximide (50 μM), and the expression of FLAG-G<sub>3</sub> and FLAG-G<sub>3s</sub> was analyzed by Western blotting after treatment at different time points.

## 2.9. Measurement of PLCβ2 Activity

G<sub>β</sub>-mediated PLC<sub>2</sub> activation was determined in COS-7 cells as described previously [29]. Briefly one day post-transfection, cells were labeled for 48 h with *myo*-[<sup>3</sup>H]inositol at 2 μCi/ml in inositol-free DMEM containing 1% dialyzed FBS. After serum starvation for 4 h, 10 mM LiCl was added to the cells to initiate inositol phosphate (IP) accumulation for 1 h. Total IPs were separated by AG 1-X8 columns and determined by  $\beta$ -spectrometry. To eliminate difference in IP accumulation caused by different cell numbers, total IPs were expressed as percentage of total [<sup>3</sup>H]-inositol incorporated into the intact cells.

## 2.10. Measurement of PI3Kγ Activity

G<sub>β</sub>-mediated PI3K<sub>γ</sub> activation assays were performed in COS-7 cells co-transfected with myc-tagged PI3K p110 and myc-tagged p101 together with FLAG-G<sub>3</sub> 2 or FLAG-G<sub>3s</sub> 2 using Lipofectamine 2000. 4 h post-transfection, the media were replaced by serum-free DMEM containing 0.1% BSA. 24 h later, cell lysates were prepared in lysis buffer containing protease inhibitors and phosphatase inhibitors (5 mM NaF, 1 mM sodium orthovanadate, 1 mM sodium pyrophosphate, 1 mM  $\beta$ -glycerophosphate, and 5 μM cantharidin). 100 μg of proteins were then subjected to SDS-PAGE and Western blotting analyses of AKT phosphorylation.

## 2.11. Measurement of ERK Activity

G<sub>β</sub>-mediated ERK activation was assessed in COS-7 cells co-transfected with HA-ERK1 and G<sub>3</sub> 2 or G<sub>3s</sub> 2, using the same procedure as the PI3K<sub>γ</sub> activation assays. 24 hr post-transfection, HA-ERK1 was immunoprecipitated with protein G Dynabeads preincubated with rat anti-HA antibody and analyzed for phosphorylation by Western blotting.

Receptor mediated ERK1/2 activation was determined in HEK293 cells transiently transfected with G<sub>3</sub> 2 or G<sub>3s</sub> 2 in the presence or absence of HA- $\beta$ 2A-adrenergic receptor ( $\beta$ 2A-AR). 24 hr post-transfection, cells were serum-starved overnight, and then stimulated with epinephrine (10 μM) in the presence of 10 μM *d,l*-propranolol for 5 min at 37°C. Cell lysates were then prepared and used for detection of ERK1/2 phosphorylation by Western blotting.

## 2.12. Measurement of PLEKHG2 Activity

HEK-293 cells seeded on 24-well plates were co-transfected with G<sub>3</sub> 2 or G<sub>3s</sub> 2 together with the pSRE-luciferase reporter plasmid and the pMaxGFP control vector. 4 hr post-transfection, cells were serum-starved overnight, washed twice with saline, and then lysed with lysis buffer (100 mM potassium phosphate, pH7.8, 0.2 % Triton X-100) containing protease inhibitors. Luciferase activities were determined using 200 μM luciferin as a substrate as described [30]. The activity of the experimental reporter was normalized against the fluorescent intensity of GFP measured with the Biotek Synergy 4 microplate reader.

### 2.13. DNA Genotyping

Genomic DNA was extracted from lymphocytic cells using Wizard genomic DNA purification kit (Promega), and used for PCR with oligonucleotide primers 5'-TGACCCACTTGCCACCCGTGC-3' (sense) and 5'-GCAGCAGCCAGGGCTGGC-3' (antisense) encompassing the genomic sequence of human G $\beta$ 3 from nucleotide 5348 to 5614. The resulting PCR amplicon was digested with *Bse*DI [10]. After *Bse*DI digestion, homozygous C825C genotypes generate bands of 115 bp and 152 bp, while homozygous C825T genotypes generate a band of 267 bp.

### 2.14. Detection of G $\beta$ 3s Transcripts

RNA was prepared from leukocytes for RT-PCR using oligonucleotide primers 5'-CGGGAGCTTTCTGCTCACAC-3' (sense) and 5'-TGTTCACTGCCTTCCACTTCC-3' (anti-sense), as described [31]. The resulting RT-PCR products encoding G $\beta$ 3 and G $\beta$ 3s are 651 bp and 528 bp, respectively. They were size-fractionated and purified from 1.5% agarose gels. The purified products were cloned onto pCR4-TOPO vector using the TOPO TA Cloning Kit (Life Technologies), followed by DNA sequencing.

### 2.15. Quantitative Real-time PCR

Relative quantification of mRNA levels in siRNA-transfected Jurkat T cells was achieved using quantitative RT-PCR (qPCR) and comparative *C<sub>t</sub>* methods. 24 hr post-transfection, total RNA was isolated from cells using Trizol (Life Technologies), and 500 ng of total RNA was reverse transcribed into cDNAs using the iScript cDNA synthesis kit (Bio-Rad). qPCR was performed using primers specific for the target gene and the iQSYBR green supermix (Bio-Rad) with the C1000 thermal cycler (Bio-Rad). mRNA expression levels of each gene were normalized with GAPDH mRNA.

### 2.16. Chemotaxis Assay

Chemotaxis of Jurkat T cells stimulated by chemoattractant SDF1 was determined as previously described [26, 29, 32].

### 2.17. Measurement of AKT, ERK1/2 phosphorylation and Cytosolic Ca<sup>2+</sup> Concentration in Jurkat T cells

AKT and ERK1/2 phosphorylation were determined by Western blotting, and the cytosolic concentration of Ca<sup>2+</sup> ([Ca<sup>2+</sup>]<sub>i</sub>) in Jurkat T cells was measured using Fura 2/AM as previously described [26, 32].

### 2.18. Statistical analysis

Data were expressed as mean  $\pm$  SE. Statistical comparisons between two groups were analyzed by two tail Student's *t* test ( $P < 0.05$  was considered significant).

## 3. Results

### 3.1. G $\beta$ 3s does not interact with either G $\gamma$ 2 or G $\alpha$ subunits

We initially attempted to purify G $\beta$ 3s for functional studies as a dimer with His-tagged G $\gamma$ 2 or G $\gamma$ 5 from Sf9 cells using nickel column but failed to achieve that, although we can easily purify G $\beta$ 3 $\gamma$ 2 or G $\beta$ 3 $\gamma$ 5 (data not shown). We verified these findings by Western blot analysis of the proteins isolated by Ni-NTA agarose (Fig. 1 A, B). Except for non-specific binding to Ni-NTA agarose, no specific binding of G $\beta$ 3s to His-G $\gamma$ 2 or His-G $\gamma$ 5 can be detected as compared to G $\beta$ 3. The failure of G $\beta$ 3s to form dimers with G $\gamma$ 2 and G $\gamma$ 5 was not due to its lower expression as G $\beta$ 3s was expressed at the similar level as G $\beta$ 3 (Fig. 1 A, B). To evaluate the possibility that the G $\beta$ 3 $\gamma$  dimer may be unstable in the presence of

detergent, we co-expressed G $\beta$ 3 or G $\beta$ 3s with a His-tagged G $\alpha$ 2 mutant (G $\alpha$ 2C68S) that is deficient in lipid modification [33], and then purified the complex from the cytosol of Sf9 cells after disrupting the cells with sonication in the absence of detergents. Although G $\beta$ 3 can be readily purified with His-G $\alpha$ 2C68S, no complex formation between G $\beta$ 3s and G $\alpha$ 2C68S can be detected (Fig. 1C). These findings suggest that G $\beta$ 3s may be deficient in the ability to interact with G $\alpha$ .

To verify the findings in mammalian cells, we co-transfected HEK293 cells with FLAG-tagged G $\beta$ 3 or G $\beta$ 3s and the HA-tagged G $\alpha$  subunits previously reported to form complexes with G $\beta$ 3 and G $\beta$ 3s [13, 23, 34], and then performed co-immunoprecipitation using an anti-HA antibody. As shown in Fig. 2A, FLAG-G $\beta$ 3 readily co-immunoprecipitated with each of G $\alpha$  subunit tested, including G $\alpha$ 2, G $\alpha$ 5, G $\alpha$ 8, G $\alpha$ 10 and G $\alpha$ 12, while FLAG-G $\beta$ 3s did not. We further investigated the interaction of G $\beta$ 3s with G $\alpha$  in intact cells, using a BRET-based assay. Co-expression of a fixed amount of pRluc-G $\beta$ 3 (donor) with increasing concentrations of pGFP $^2$ -G $\alpha$ 5 or pGFP $^2$ -G $\alpha$ 8 (acceptor) led to a dose-dependent increase in net BRET values that are significantly larger than those observed with the co-expression of pRluc-G $\beta$ 3 with the control pGFP $^2$  alone (Fig. 2B). In contrast, when BRET was measured between pRluc-G $\beta$ 3s and pGFP $^2$ -G $\alpha$ 5 or pGFP $^2$ -G $\alpha$ 8, the net BRET values were not significantly different from that between pRluc-G $\beta$ 3s and pGFP $^2$  (Fig. 2C). Similar results were observed when pRluc-G $\beta$ 3 or pRluc-G $\beta$ 3s was co-expressed with a single saturation concentration of pGFP $^2$ -G $\alpha$ 2, pGFP $^2$ -G $\alpha$ 10 or pGFP $^2$ -G $\alpha$ 12 (Fig. 2D). Taken together, these data demonstrate that, as compared to G $\beta$ 3, G $\beta$ 3s lacks the ability to form a complex with G $\alpha$  subunits.

It has been shown previously that expression of G $\beta$ 3s facilitated an increase in GTP $\gamma$ S binding to G $\alpha$  subunits stimulated by the activating peptide mastoparan 7 or GPCRs, implying that G $\beta$ 3s can interact with G $\alpha$  subunits [10, 23]. To directly examine the interaction of G $\beta$ 3s with G $\alpha$  subunits, we immunoprecipitated FLAG-G $\beta$ 3 or FLAG-G $\beta$ 3s from HEK293 cell lysates after co-expression with G $\alpha$ 2, and then examined the immunoprecipitates for the presence of endogenous G $\alpha$  subunits by Western blot. Although there was no interaction with G $\alpha$ s, FLAG-G $\beta$ 3 co-immunoprecipitated with G $\alpha$ i, G $\alpha$ q/11 and G $\alpha$ 12. In contrast, none of these G $\alpha$  subunits was detected in the FLAG-G $\beta$ 3s immunoprecipitate (Fig. 3). These findings indicate that G $\beta$ 3s is also deficient in interaction with G $\alpha$  subunits.

### 3.2. G $\beta$ 3s displayed altered cellular localization and a decreased stability

The association of G $\beta$  with G $\alpha$  and G $\gamma$  is known to facilitate the membrane localization of G $\beta$  [33, 35]. Given that G $\beta$ 3s fails to bind either G $\alpha$  or G $\gamma$  subunits, it raises the possibility that it may not localize properly to the cell membrane. To test this, we generated stable HEK293 cell lines expressing comparable levels of FLAG-G $\beta$ 3 and FLAG-G $\beta$ 3s. As expected, like the endogenous G $\beta$ , FLAG-G $\beta$ 3 is located primarily in the plasma membrane (Fig. 4A). In contrast, FLAG-G $\beta$ 3s is diffusely distributed in the cytosol (Fig. 4A).

The association of G $\beta$  with G $\alpha$  is also known to render the stability of G $\beta$  [36]. Therefore, we further investigated if the deficiency of G $\beta$ 3s in forming a complex with G $\alpha$  subunits affects its stability. We treated HEK293 cells stably expressing FLAG-G $\beta$ 3 and FLAG-G $\beta$ 3s with the protein synthesis inhibitor cycloheximide (CHX) for different amount of time (0-8 hr) and then analyzed the level of proteins by Western blotting. While more than 80% of FLAG-G $\beta$ 3 remained detectable 8 hr after CHX treatment, FLAG-G $\beta$ 3s rapidly degraded in 0.5 hr and became almost undetectable in 8 hr (Fig. 4B). The calculated half-life of FLAG-G $\beta$ 3 and FLAG-G $\beta$ 3s turnover is 18 hr *versus* 0.3 hr.

### 3.3. Gβ3s does not activate Gβγ effectors

We next determined whether G<sub>3s</sub> is capable of stimulating G<sub>βγ</sub>-dependent effectors. We first evaluated the well-described canonical G<sub>βγ</sub> effectors, PLC<sub>2</sub>, ERK1/2 and PI3K. As shown in Fig. 5A, co-expression of G<sub>3 2</sub> with PLC<sub>2</sub> in COS-7 cells dose dependently increased PLCB2 activity 2-5 fold above basal. In contrast, when G<sub>3s</sub> was co-expressed with G<sub>2</sub> at the similar level as G<sub>3</sub>, the activity of PLC<sub>2</sub> was not significantly increased. Similar data were obtained with the activation of PLC<sub>3</sub> (data not shown). Similarly, while overexpression of G<sub>3 2</sub> led to increased phosphorylation of the co-expressed HA-ERK1, and PI3K-mediated phosphorylation of endogenous AKT, overexpression of G<sub>3s 2</sub> had no effects (Fig. 5B, C). The failure of G<sub>3s</sub> to activate various effectors was not due to its low expression, as the level of G<sub>3s</sub> expression was comparable to that of G<sub>3</sub>.

We then examined whether G<sub>3s</sub> can activate a recently discovered G<sub>βγ</sub> effector, PLEKHG2, a RhoGEF [37]. To monitor PLEKHG2 activity, we measured transcription of a reporter gene, luciferase, controlled by the SRE promoter, which is known to be regulated by RhoGTPases [38]. Co-expression of G<sub>3 2</sub> stimulated PLEKHG2-induced luciferase activity in a dose-dependent manner (Fig. 5D), but co-expression of G<sub>3s 2</sub> had no effects on PLEKHG2 activity (Fig. 5D).

### 3.4. Gβ3s does not modulate GPCR signaling

Heterologous expression of G<sub>3s</sub> has been shown to enhance GPCR-stimulated GTP binding on G<sub>β</sub> subunits and cell migration, implying that G<sub>3s</sub> may facilitate increased coupling of heterotrimeric G proteins to GPCRs for signal transduction [13, 23, 39]. To test this, we examined if overexpression of G<sub>3</sub> or G<sub>3s</sub> affects ERK1/2 phosphorylation stimulated by co-expressed 2A-AR in HEK293 cells. The 2A-AR stimulated ERK1/2 phosphorylation via G<sub>β</sub> released from the activated Gi/o proteins, because it is sensitive to inhibition by pertussis toxin treatment or overexpression of G<sub>βt</sub> that sequesters free G<sub>β</sub> (data not shown) [29]. Overexpression of either G<sub>3 2</sub> or G<sub>3s 2</sub> did not affect 2A-AR-stimulated ERK1/2 phosphorylation (Fig. 6), suggesting that neither G<sub>3</sub> nor G<sub>3s</sub> is able to enhance 2A-AR-mediated signal transduction. Similar results were found when LPA-stimulated ERK1/2 phosphorylation via endogenous LPA receptors was tested (data not shown).

### 3.5. Gβ3s protein is undetectable in human lymphocytic cell lines expressing Gβ3s transcript

To further understand the function of G<sub>3s</sub>, we screened several human leukocyte cell lines for the presence of G<sub>3</sub> C825T polymorphism and the expression of endogenous G<sub>3s</sub> transcripts. As reported [10], we genotyped the cell lines for the presence of C825T by PCR followed by restriction enzyme digestion (Fig. 7A). We identified homozygous C825C and T825T alleles in B lymphocytic cell lines GM19116C and GM18500B, respectively, and heterozygous C825T allele in Jurkat T cell line. As reported previously [31], RT-PCR analysis followed by DNA sequencing of the RT-PCR product indicate that G<sub>3s</sub>-specific mRNA transcript was expressed only in cell lines containing the T825 allele, while the wild-type G<sub>3</sub> mRNA transcript can be detected in all cell lines regardless of the T825 status (Fig. 7B). To determine the expression of G<sub>3s</sub> protein, we used a pan anti-G<sub>β</sub> antibody (T20) that recognizes G<sub>1</sub>, G<sub>2</sub>, G<sub>3</sub>, G<sub>3s</sub>, and G<sub>4</sub> but not G<sub>5</sub> by Western blotting (Fig. 7C), since we could not identify a commercially available antibody that recognizes G<sub>3</sub> and G<sub>3s</sub> specifically (data not shown). Using this antibody, we detected expression of endogenous G<sub>β</sub> in all cell lines, but could not detect a protein corresponding to the size of G<sub>3s</sub> in the cell lines expressing G<sub>3s</sub> mRNA transcripts (Fig. 7D). These findings are consistent with the notion that G<sub>3s</sub> is an unstable protein, but does not exclude the



possibility that low levels of G<sub>3s</sub> expression may also occur at the translational and transcription level.

### 3.6. G<sub>β3</sub> does not play a role in transmitting chemotactic signal for leukocyte migration

Given our data indicating that G<sub>3s</sub> is an unstable and functionally inactive protein, it is likely that the pathological effects of G<sub>3</sub> C825T result from the downregulation of G<sub>3</sub> function, and not the enhanced functionality of G<sub>3s</sub>. To test this, we further evaluated the role of G<sub>3</sub> in mediating chemotaxis in human lymphocytic cell lines, as leukocytes from individuals carrying G<sub>3</sub> C825T have been shown to exhibit enhanced chemotactic responses to chemoattractant stimulation. We initially chose Jurkat T cells as a model system for studies because this cell line expresses a substantial amount of G<sub>3</sub>, although it contains heterozygous C825T allele and also expresses G<sub>3s</sub> transcripts (Fig. 7A, B). Moreover, Jurkat T cells exhibit robust chemotactic and signaling responses after stimulation with SDF1. We transiently transfected Jurkat T cells with a siRNA to specifically inhibit G<sub>3</sub> and G<sub>3s</sub> expression (Fig. 8A). Downregulation of G<sub>3</sub> and G<sub>3s</sub> had no effect on SDF1-stimulated Ca<sup>2+</sup> signaling and AKT and ERK phosphorylation, nor did it affect SDF1-stimulated chemotaxis (Fig. 8B, C). These findings indicate that G<sub>3</sub> and G<sub>3s</sub> do not play a major role in SDF1-stimulated signal transduction and Jurkat T cell migration. In supporting this notion, transfection of Jurkat T cells with a siRNA targeting a common sequence shared by G<sub>1</sub> and G<sub>2</sub> alleviated SDF1-activated Ca<sup>2+</sup> signaling, AKT and ERK phosphorylation, and completely abolished SDF1-stimulated cell migration (Fig. 8C, D). In contrast, OKT3-stimulated Ca<sup>2+</sup> signaling via T cell receptors was not affected, indicating that inhibition of G<sub>1</sub> and G<sub>2</sub> specifically affects GPCR-mediated signal transduction (Fig. 8B, C). Notably, targeting either G<sub>1</sub> or G<sub>2</sub> alone had no effect, indicating that the function of SDF1 is mediated primarily via G<sub>1</sub> and G<sub>2</sub> and that these two G isoforms have a redundant role in Jurkat T cells (data not shown).

To determine if G<sub>3</sub> has a cell type-specific function, we further evaluated its role in GM19116C cells, a B lymphocytic cell line that contains homozygous C825C allele and expresses only G<sub>3</sub> (Fig. 7A, B). As with Jurkat T cells, inhibition of G<sub>3</sub> had no effect on SDF1-induced cell migration, while targeting G<sub>1</sub> and G<sub>2</sub> abolished chemotaxis (Fig. 8E). Together, these data indicate that G<sub>3</sub> does not play a major role in mediating SDF1-stimulated signal transduction and lymphocyte migration.

## 4. Discussion

In this study, we have provided unambiguous evidence that the splice variant of G<sub>3</sub> associated with C825T polymorphism is a functionally inactive protein. We show that, unlike a canonical G protein, G<sub>3s</sub> does not form a dimer with G<sub>2</sub> after heterologous overexpression in a mammalian or an insect system. The deficiency in dimerization of G<sub>3s</sub> and G<sub>2</sub> cannot be explained by instability caused by detergents, which has been previously reported for certain G isoforms such as G<sub>5</sub> [40]. This is evident from data showing that G<sub>3s</sub> does not form a dimer with a G<sub>2</sub> mutant deficient in lipid modification in lysis buffer containing no detergents, nor does it interact with various G<sub>1</sub> in intact cells as determined by the BRET-based assays. Co-immunoprecipitation analyses also showed that, unlike G<sub>3</sub>, G<sub>3s</sub> does not interact with various G<sub>α</sub> subunits. Given that G<sub>β</sub> subunits are obligate partners of G<sub>α</sub> subunits, it is not surprising that G<sub>3s</sub> does not activate diverse G<sub>α</sub> effectors, including the classical effectors, PLC 2/3, PI3K /AKT and ERKs, and the newly identified effector, the RhoGEF PLEKHG2. These findings are consistent with the report of Ruiz-Velasco et al. that G<sub>3s</sub> does not form a dimer with G<sub>2</sub> as determined by fluorescence resonance energy transfer measurements, and does not modulate N-type Ca<sup>2+</sup> or G protein-gated inwardly rectifying K<sup>+</sup> channels when it was co-expressed with G<sub>2</sub> or G<sub>5</sub> in rat

sympathetic neurons [24]. Our failure to purify G<sub>3s</sub> as a dimer with either G<sub>2</sub> or G<sub>5</sub> from the Sf9 cell expression system is also supported by the reports of other groups [23, 41, 42].

G<sub>3</sub> belongs to the superfamily of WD40 repeat-containing proteins. Its C-terminus consists of seven WD40 repeat domains that form a toroidal seven-bladed propeller structure with each propeller comprising four anti-parallel sheets [43]. Each WD40 repeat forms part of two blades within a propeller, including the outer strand of one blade and the three inner strands of another. G<sub>3s</sub> lacks the entire fourth WD40 repeat domain [10]. Based on sequence analyses, WD40 proteins are predicted to contain 4-16 WD40 repeats [44]. Therefore, it has been proposed that despite the lack of one WD40 repeat, G<sub>3s</sub> can still form a stable six-blade propeller structure [13]. However, if this is the case, G<sub>3s</sub> should still be able to interact with G<sub>β</sub> because a majority of residues involved in binding G<sub>β</sub> are still retained in the N-terminal coiled helix and the WD40 domains 5-7 of G<sub>3s</sub> [43]. The fact that G<sub>3s</sub> is deficient in forming a complex with G<sub>α</sub> and G<sub>γ</sub> indicates that the remaining six WD40 domains of G<sub>3s</sub> are unable to form a stable propeller structure. This notion is consistent with modeling prediction that a seven-fold symmetry is preferable to six- or eight-fold symmetry for propeller assembly [45], and our findings that G<sub>3s</sub> is highly unstable as compared to G<sub>3</sub>.

Our findings that G<sub>3s</sub> is a functionally inactive protein contradict the reports by Siffert's group. They initially proposed that G<sub>3s</sub> was a functional protein because it was identified in lymphocytes derived from patients with essential hypertension that showed increased G<sub>β</sub> protein signaling, and it has the same ability as G<sub>3</sub> to support MAS-7-stimulated GTP<sub>s</sub> binding to G<sub>β</sub> when co-expressed with G<sub>αi2</sub> and G<sub>γ5</sub> in Sf9 cells [10]. Using the same assay, they later showed that, as compared to G<sub>3</sub>, G<sub>3s</sub> displayed an increased ability to mediate receptor-stimulated GTP<sub>s</sub> binding to G<sub>β</sub> [23]. Moreover, overexpression of G<sub>3s</sub> alone was sufficient to increase MAS-7-stimulated GTP<sub>s</sub> binding in permeabilized COS-7 cells [23]. COS-7 overexpressing G<sub>3s</sub> also showed enhanced chemotactic response to LPA stimulation [39]. However, these studies did not directly determine whether G<sub>3s</sub> indeed formed a heterotrimeric complex with the co-expressed G<sub>αi2</sub> and G<sub>γ5</sub>. Our co-immunoprecipitation studies provided the direct evidence that unlike G<sub>3</sub>, G<sub>3s</sub> lacks the ability to form a complex with endogenous G<sub>β</sub> subunits in HEK293 cells.

Siffert's group also reported that G<sub>3s</sub> can form dimers with various G<sub>β</sub> after they were translated *in vitro* or co-expressed in HEK293 cells, followed by immunoprecipitation of G<sub>β</sub> [13, 23]. However, the amount of G<sub>3s</sub> co-immunoprecipitated with G<sub>β</sub> was much less than that of G<sub>3</sub>. Moreover, as we found here, they also showed that no G<sub>3s</sub> could be co-purified with G<sub>β</sub> from Sf9 cells [23]. Given our findings that G<sub>3s</sub> is unstable, it is likely that the small amount of G<sub>3s</sub> co-immunoprecipitated with G<sub>β</sub> may represent the unstable G<sub>3s</sub> protein precipitated from solution.

Based on the findings that overexpression of G<sub>3s</sub> alone was sufficient to significantly enhance the activity of co-expressed ERK1 as compared to G<sub>3</sub>, Siffert's group proposed that G<sub>3s</sub> is a gain-of-function protein [13]. However, in the same study it was found that G<sub>3s</sub>, expressed either alone or in combination with G<sub>γ</sub>, was unable to stimulate PLC<sub>2</sub>. It was recently found that G<sub>3</sub> preferentially activates PLC<sub>3</sub> over PLC<sub>2</sub> [34]. Nevertheless, we found that G<sub>3s</sub> is deficient in stimulating either PLC<sub>3</sub> or PLC<sub>2</sub>. Moreover, G<sub>3s</sub> is unable to activate several other G<sub>β</sub> effectors. Together with the findings that overexpression of G<sub>3s</sub> does not affect GPCR-mediated signal transduction, our data strongly indicate that G<sub>3s</sub> is a loss-of-function protein.

The idea that G<sub>3s</sub> is a gain-of-function protein has become the dogma in the field of G<sub>3</sub> polymorphisms, and has been and continues to be used as the mechanistic basis for the

association of G<sub>3</sub> C825T allele with diverse pathophysiological effects in many studies in the literature [14]. However, many of these studies examined neither the expression nor the direct contribution of G<sub>3</sub>s to the described effects. Our findings that G<sub>3</sub>s is an unstable and functionally inactive protein indicate that the potential mechanisms associated with G<sub>3</sub> C825T allele are probably due to downregulation of the expression and function of G<sub>3</sub>. Therefore, to fully understand the effect of the G<sub>3</sub> C825T polymorphism, it is critical to evaluate the expression level of G<sub>3</sub> in the carriers of different genotypes and to define the functionality of G<sub>3</sub>. Based on Northern blotting analyses, G<sub>3</sub> was shown to be widely expressed in many tissues [46]. The expression of G<sub>3</sub> protein in several cell types and multiple regions of adult rat brain was also shown by Western blot and immunohistochemistry analyses [10, 47, 48]. It was also reported that the expression of G<sub>3</sub> was decreased in the adipocytes of G<sub>3</sub> C825T carriers [47]. However, the specificity of G<sub>3</sub> antibodies used in these studies was not well characterized. G<sub>3</sub> shares a high degree of homology in amino acid sequences to other G<sub>3</sub> isoforms, and consequently, it is hard to identify a region of G<sub>3</sub> with amino acid sequences divergent enough to other G<sub>3</sub> isoforms for preparing G<sub>3</sub> specific antibodies. Indeed, we found that many commercially available antibodies that are claimed to specifically recognize G<sub>p3</sub> can also detect other G<sub>3</sub> isoforms (data not shown). Thus, future studies are required to develop specific antibodies for G<sub>3</sub> or other approaches to further characterize the distribution of G<sub>3</sub> in tissues.

Accumulating evidence indicates that distinct combinations of different isoforms of G<sub>1</sub>, G<sub>2</sub> and G<sub>3</sub> may determine the signaling specificity of GPCRs [1, 9]. For example, it has been shown that the mouse macrophage cell line J774A.1 expresses G<sub>1</sub>, G<sub>2</sub> and G<sub>4</sub> isoforms, but G<sub>2</sub> was the primary G<sub>3</sub> subunit that mediates the signaling and function of the C5a receptor in this cell line [49]. By using antisense oligonucleotides against different G<sub>3</sub> isoforms, it has been established that G<sub>1</sub> and G<sub>3</sub> subunits selectively mediate the effect of the somatostatin and muscarinic receptors, respectively, to inhibit the voltage-sensitive Ca<sup>2+</sup> channels [50]. Based on findings that platelets, neutrophils, T lymphocytes and coronary arteries from carriers with G<sub>3</sub> C825T allele displayed enhanced responses to GPCR stimulation, it has been suggested that G<sub>3</sub>s plays a positive role in regulating functions of these cells, although direct evidence is still lacking [39, 51-53]. Our data show that although G<sub>3</sub> and G<sub>3</sub>s transcripts are detected in human lymphocytic cell lines containing G<sub>3</sub> C825T allele, SDF1 $\alpha$ -stimulated signaling and chemotactic response are not mediated by G<sub>3</sub> and G<sub>3</sub>s, but rather, by the redundant function of G<sub>1</sub> and G<sub>2</sub> in these cells. These findings indicate that the role of G<sub>3</sub> in mediating cell signaling and function likely depends on the receptors and the cell types. Thus, the reported association of G<sub>3</sub> C825T polymorphism with various disorders in different organs should be interpreted with great caution. Given that the conversion of G<sub>3</sub> to G<sub>3</sub>s results in the loss of G<sub>3</sub> function, clearly, to comprehend the functionality of G<sub>3</sub> C825T polymorphism, future work is required to further characterize the role of G<sub>3</sub> in mediating the function of diverse GPCRs in different cells and tissues.

## 5. Conclusions

In conclusion, we results demonstrate that the splice variant of G<sub>3</sub>, G<sub>3</sub>s, is a structurally unstable and functionally inactive protein. Moreover, we provided evidence that the role of G<sub>3</sub> in mediating functions of GPCRs is likely to be stimuli and/or tissue specific.

## Acknowledgments

The work was supported in part by American Heart Association grant 10GRNT3620015 (to S.C.), and National Institute of Health Grant GM094255 (to S.C.).

## References

1. Oldham WM, Hamm HE. *Nat Rev Mol Cell Biol.* 2008; 9:60–71. [PubMed: 18043707]
2. Tesmer JJ. *Nature structural & molecular biology.* 2010; 17:650–652.
3. Vassart G, Costagliola S. *Nature reviews Endocrinology.* 2011; 7:362–372.
4. Thathiah A, De Strooper B. *Nature reviews Neuroscience.* 2011; 12:73–87.
5. Brinks HL, Eckhart AD. *Biochim Biophys Acta.* 2010; 1802:1268–1275. [PubMed: 20060896]
6. Lappano R, Maggiolini M. *Nature reviews Drug discovery.* 2011; 10:47–60.
7. Tiwari A. *Current opinion in investigational drugs.* 2010; 11:385–393. [PubMed: 20336586]
8. Whalen EJ, Rajagopal S, Lefkowitz RJ. *Trends in molecular medicine.* 2011; 17:126–139. [PubMed: 21183406]
9. Smrcka AV. *Cellular and molecular life sciences: CMLS.* 2008; 65:2191–2214. [PubMed: 18488142]
10. Siffert W, Roszkopf D, Siffert G, Busch S, Moritz A, Erbel R, Sharma AM, Ritz E, Wichmann HE, Jakobs KH, Horsthemke B. *Nature genetics.* 1998; 18:45–48. [PubMed: 9425898]
11. Roszkopf D, Busch S, Manthey I, Siffert W. *Hypertension.* 2000; 36:33–41. [PubMed: 10904009]
12. Roszkopf D, Kielbik M, Manthey I, Bilmen G, Eisenhardt A, Siffert W. *Biochim Biophys Acta.* 2003; 1626:33–42. [PubMed: 12697327]
13. Roszkopf D, Manthey I, Habich C, Kielbik M, Eisenhardt A, Nikula C, Urban M, Kohlen S, Graf E, Ravens U, Siffert W. *Biochem J.* 2003; 371:223–232. [PubMed: 12431187]
14. Klenke S, Kussmann M, Siffert W. *Pharmacogenetics and genomics.* 2011; 21:594–606. [PubMed: 21709600]
15. Siffert W. *Annual review of medicine.* 2005; 56:17–28.
16. Lopez-Leon S, Janssens AC, Gonzalez-Zuloeta Ladd AM, Del-Favero J, Claes SJ, Oostra BA, van Duijn CM. *Molecular psychiatry.* 2008; 13:772–785. [PubMed: 17938638]
17. Sheu SY, Handke S, Brocker-Preuss M, Gorges R, Frey UH, Ensinger C, Ofner D, Farid NR, Siffert W, Schmid KW. *The Journal of pathology.* 2007; 211:60–66. [PubMed: 17136758]
18. Holmen OL, Romundstad S, Melien O. *American journal of hypertension.* 2010; 23:1121–1127. [PubMed: 20539277]
19. Plat AW, Stoffers HE, Klungel OH, van Schayck CP, de Leeuw PW, Soomers FL, Schiffers PM, Kester AD, Kroon AA. *Journal of human hypertension.* 2009; 23:659–667. [PubMed: 19242491]
20. Kato M, Wakeno M, Okugawa G, Fukuda T, Takekita Y, Hosoi Y, Azuma J, Kinoshita T, Serretti A. *Progress in neuro-psychopharmacology & biological psychiatry.* 2008; 32:1041–1044. [PubMed: 18325652]
21. Kurnik D, Muszkat M, Sofowora GG, Friedman EA, Dupont WD, Scheinin M, Wood AJ, Stein CM. *Hypertension.* 2008; 51:406–411. [PubMed: 18071056]
22. Meirhaeghe A, Cotel D, Amouyel P, Dallongeville J. *Molecular genetics and metabolism.* 2005; 86:293–299. [PubMed: 15978856]
23. Roszkopf D, Koch K, Habich C, Geerdes J, Ludwig A, Wilhelms S, Jakobs KH, Siffert W. *Cell Signal.* 2003; 15:479–488. [PubMed: 12639711]
24. Ruiz-Velasco V, Ikeda SR. *Physiological genomics.* 2003; 13:85–95. [PubMed: 12595577]
25. Dingus J, Wells CA, Campbell L, Cleator JH, Robinson K, Hildebrandt JD. *Biochemistry.* 2005; 44:11882–11890. [PubMed: 16128590]
26. Sun Z, Tang X, Lin F, Chen S. *J Biol Chem.* 286:43902–43912. [PubMed: 22065575]
27. Pflieger KD, Seeber RM, Eidne KA. *Nat Protoc.* 2006; 1:337–345. [PubMed: 17406254]
28. Oner SS, An N, Vural A, Breton B, Bouvier M, Blumer JB, Lanier SM. *J Biol Chem.* 2010; 285:33949–33958. [PubMed: 20716524]
29. Chen S, Dell EJ, Lin F, Sai J, Hamm HE. *J Biol Chem.* 2004; 279:17861–17868. [PubMed: 14963031]
30. Hampf M, Gossen M. *Anal Biochem.* 2006; 356:94–99. [PubMed: 16750160]
31. Virchow S, Ansorge N, Rubben H, Siffert G, Siffert W. *FEBS Lett.* 1998; 436:155–158. [PubMed: 9781669]

32. Chen S, Lin F, Shin ME, Wang F, Shen L, Hamm HE. *Mol Biol Cell*. 2008; 19:3909–3922. [PubMed: 18596232]
33. Muntz KH, Sternweis PC, Gilman AG, Mumby SM. *Mol Biol Cell*. 1992; 3:49–61. [PubMed: 1550955]
34. Poon LS, Chan AS, Wong YH. *Cell Signal*. 2009; 21:737–744. [PubMed: 19168127]
35. Takida S, Wedegaertner PB. *J Biol Chem*. 2003; 278:17284–17290. [PubMed: 12609996]
36. Higgins JB, Casey PJ. *J Biol Chem*. 1994; 269:9067–9073. [PubMed: 8132644]
37. Ueda H, Nagae R, Kozawa M, Morishita R, Kimura S, Nagase T, Ohara O, Yoshida S, Asano T. *J Biol Chem*. 2008; 283:1946–1953. [PubMed: 18045877]
38. Hill CS, Wynne J, Treisman R. *Cell*. 1995; 81:1159–1170. [PubMed: 7600583]
39. Virchow S, Ansorge N, Rosskopf D, Rubben H, Siffert W. *Naunyn Schmiedebergs Arch Pharmacol*. 1999; 360:27–32. [PubMed: 10463330]
40. Jones MB, Garrison JC. *Anal Biochem*. 1999; 268:126–133. [PubMed: 10036171]
41. McIntire WE, MacCleery G, Garrison JC. *J Biol Chem*. 2001; 276:15801–15809. [PubMed: 11278863]
42. Maier U, Babich A, Macrez N, Leopoldt D, Gierschik P, Illenberger D, Nurnberg B. *J Biol Chem*. 2000; 275:13746–13754. [PubMed: 10788495]
43. Sondak J, Bohm A, Lambright DG, Hamm HE, Sigler PB. *Nature*. 1996; 379:369–374. [PubMed: 8552196]
44. Smith TF, Gaitatzes C, Saxena K, Neer EJ. *Trends Biochem Sci*. 1999; 24:181–185. [PubMed: 10322433]
45. Murzin AG. *Proteins*. 1992; 14:191–201. [PubMed: 1409568]
46. Ansari-Lari MA, Muzny DM, Lu J, Lu F, Lilley CE, Spanos S, Malley T, Gibbs RA. *Genome Res*. 1996; 6:314–326. [PubMed: 8723724]
47. Ryden M, Faulds G, Hoffstedt J, Wennlund A, Arner P. *Diabetes*. 2002; 51:1601–1608. [PubMed: 11978662]
48. Liang JJ, Cockett M, Khawaja XZ. *J Neurochem*. 1998; 71:345–355. [PubMed: 9648884]
49. Hwang, JI.; Fraser, ID.; Choi, S.; Qin, XF.; Simon, MI. *Proceedings of the National Academy of Sciences of the United States of America*; 2004; p. 488-493.
50. Kleuss C, Scherubl H, Hescheler J, Schultz G, Wittig B. *Nature*. 1992; 358:424–426. [PubMed: 1322501]
51. Baumgart D, Naber C, Haude M, Oldenburg O, Erbel R, Heusch G, Siffert W. *Circulation research*. 1999; 85:965–969. [PubMed: 10559144]
52. Naber C, Hermann BL, Vietzke D, Altmann C, Haude M, Mann K, Rosskopf D, Siffert W. *FEBS Lett*. 2000; 484:199–201. [PubMed: 11078878]
53. Lindemann M, Virchow S, Ramann F, Barsegian V, Kreuzfelder E, Siffert W, Muller N, Grosse-Wilde H. *FEBS Lett*. 2001; 495:82–86. [PubMed: 11322952]

## Abbreviations

<b>BRET</b>	Bioluminescence resonance energy transfer
<b>GPCR</b>	G protein-coupled receptor
<b>IP</b>	inositol phosphate
<b>PTx</b>	pertussis toxin
<b>RhoGEF</b>	Rho guanine exchange factor

**Highlights**

- G 3s is deficient in interacting with G and G .
- G 3s is structurally unstable and fails to localize properly to cell membranes.
- No G 3s protein can be detected in human lymphocytes expressing its transcript
- G 3s fails to active diverse G effectors

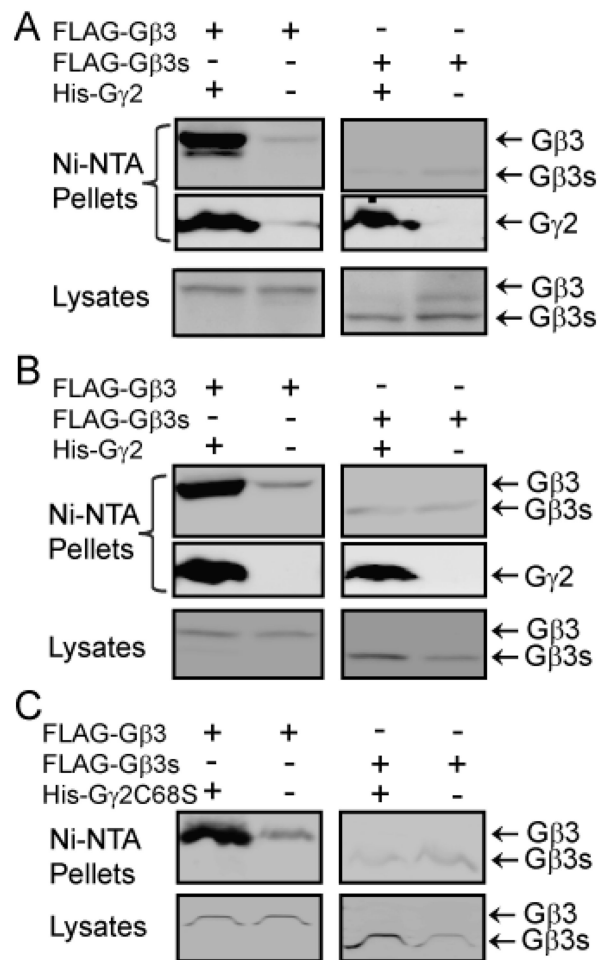


**Figure 1. G $\beta$ 3s does not form dimers with G $\beta$ 3 in Sf9 cells**

Sf9 cells were infected with baculoviruses encoding FLAG-G $\beta$ 3 or FLAG-G $\beta$ 3s together with baculoviruses encoding His-G $\gamma$ 2, His-G $\gamma$ 5 or His-G $\gamma$ 2C68S mutant. 72 hr post-infection, proteins were isolated with Ni-NTA agarose in the presence (A-B) or absence of the detergent Genapol C-100 (C), and detected by anti-FLAG and anti-His antibodies. Representative images from more than three independent experiments are shown.

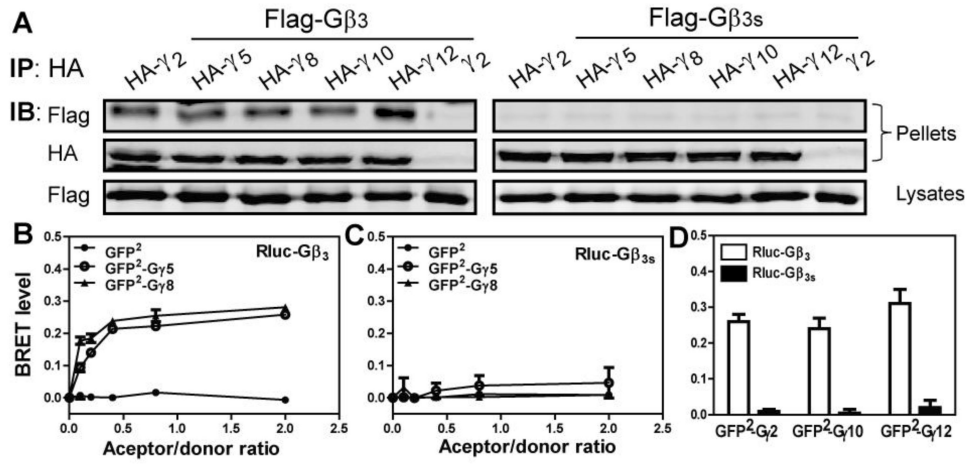


**Figure 2. G 3s does not form dimers with G in HEK293 cells**

A, FLAG-G 3 and FLAG-G 3s were co-transfected with the indicated HA-tagged G isoforms or untagged G 2 in HEK293 cells. Immunoprecipitation assays were performed by anti-HA antibody followed by Western blotting. Representative images from three independent experiments are shown. B-D, HEK293 cells were transfected with a fixed amount of Rlu-G 3 (100 ng) or Rlu-G 3s (150 ng) and increasing concentration (0-300 ng) of GFP<sup>2</sup>, GFP<sup>2</sup>-G 2, GFP<sup>2</sup>-G 5 (B-C), or a fixed concentration (300 ng) of GFP<sup>2</sup>-G 2, GFP<sup>2</sup>-G 10 or GFP<sup>2</sup>-G 12 (D), and processed for BRET measurement as described under “Experimental Procedures”. Results are expressed as the mean ± S.E. (n=3-5).



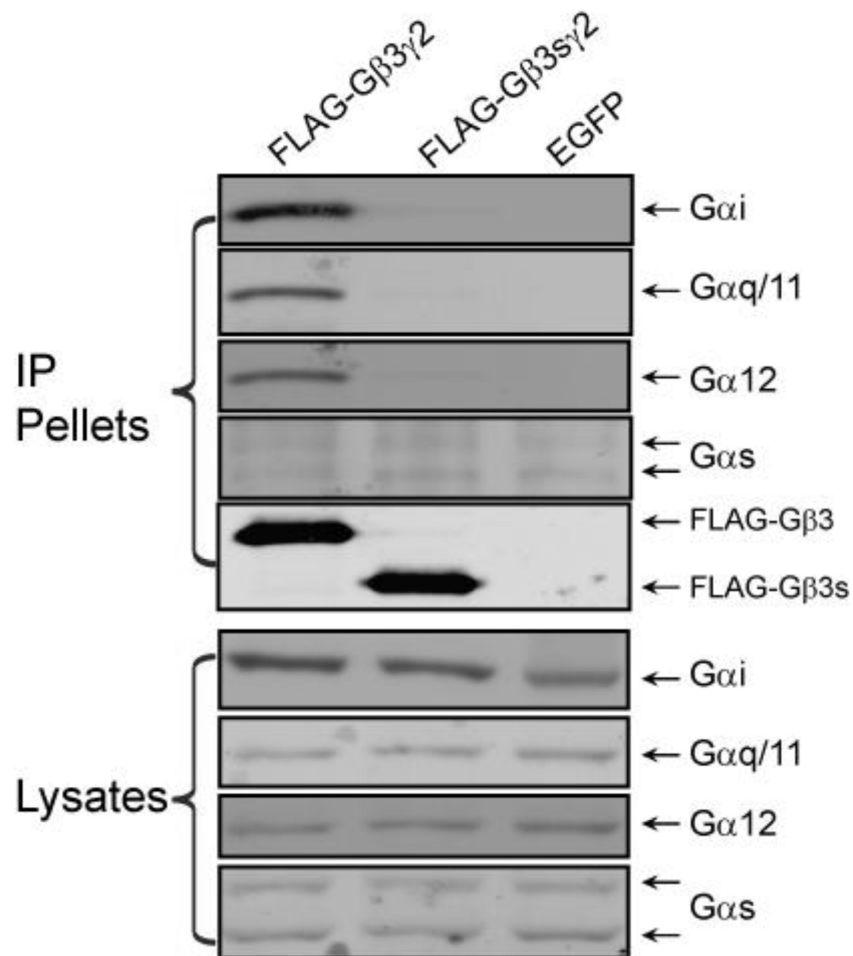


**Figure 3. G $\alpha$ 3s does not interact with endogenous G $\alpha$  in HEK293 cells**  
 HEK293 cells were co-transfected with EGFP, FLAG-G $\beta$ 3 or FLAG-G $\beta$ 3s together with HA-G $\beta$ 2 and processed for immunoprecipitation with an anti-FLAG antibody. Endogenous G $\alpha$  subunits co-immunoprecipitated with FLAG-G $\beta$ 3 and FLAG-G $\beta$ 3s were detected with specific antibodies. Representative images from more than three independent experiments are shown.

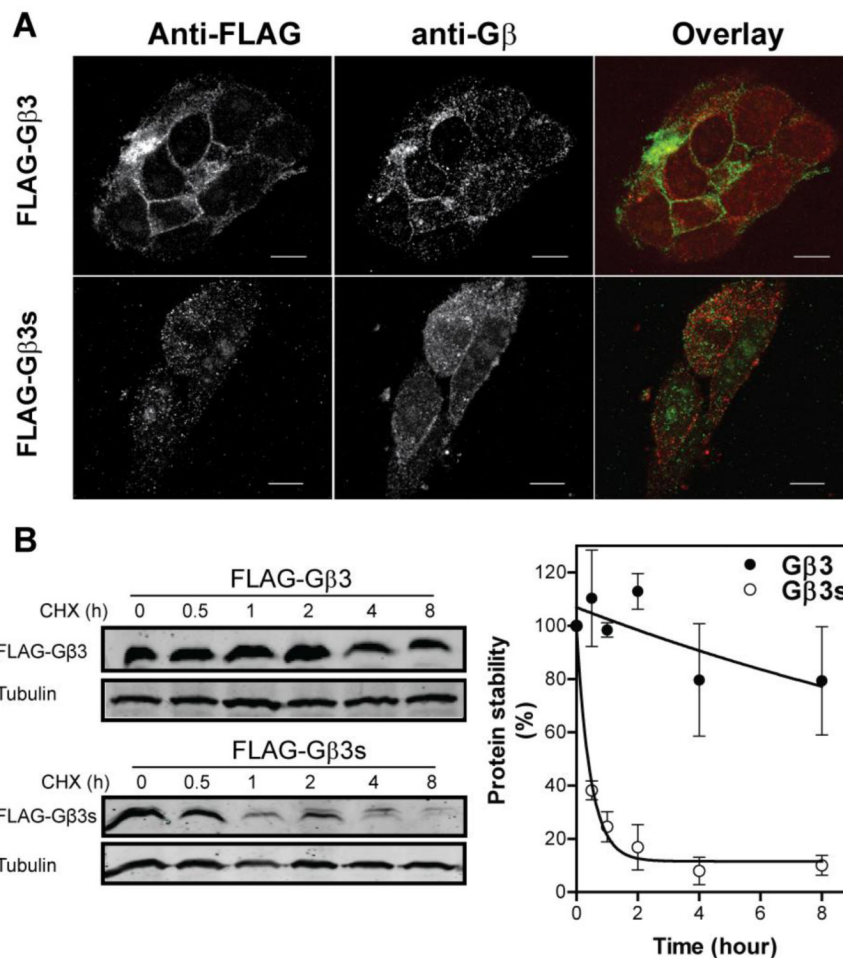


**Figure 4. Localization and stability of G $\beta$ 3 and G $\beta$ 3s in HEK293 cells**

**A**, The cellular localization of FLAG-G $\beta$ 3, FLAG-G $\beta$ 3s and endogenous G $\beta$  in HEK293 cells stably expressing FLAG-G $\beta$ 3 and FLAG-G $\beta$ 3s was revealed by staining with a mouse anti-FLAG and a rabbit pan anti-G $\beta$  antibodies followed by an Alexa488-conjugated anti-mouse and an Alex568-conjugated anti-rabbit IgG secondary antibodies. The images are the representatives of more than 20 cells from at least three separate experiments with similar results. **B**, The stability of FLAG-G $\beta$ 3 and FLAG-G $\beta$ 3s stably expressed in HEK293 cells was determined by treatment with cycloheximide for different amount of time (0-8 hr), followed by Western blotting analyses of protein expression. Displayed are representative images and quantitative data from at least three separate experiments expressed as the mean  $\pm$  S.E. \*  $p < 0.05$  indicate significance *versus* control.

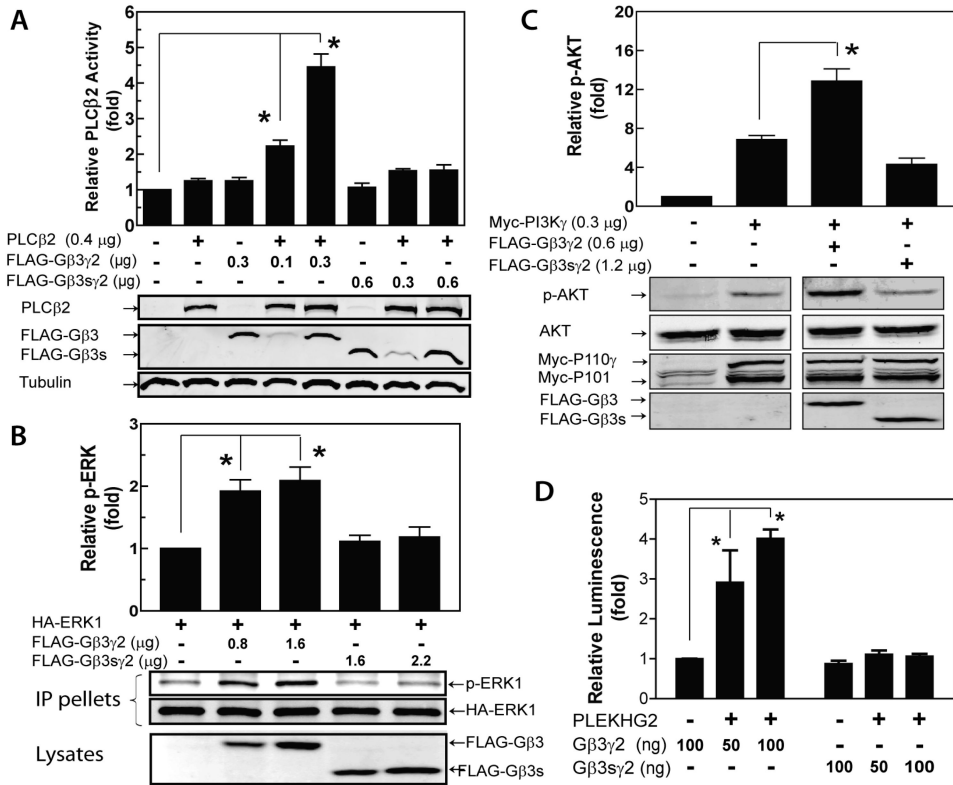


**Figure 5. G 3s does not activate diverse G effectors**

**A**, PLC 2 activation. Total inositol phosphates were measured in COS7 cells transfected with the indicated concentration of vectors encoding PLC 2 together with FLAG-G 3 2 or FLAG-G 3s 2. **B**, ERK activation. COS7 cells were transfected with HA-ERK1 together with FLAG-G 3 2 or FLAG-G 3s 2 as indicated. 24 hr post-transfection, HA-ERK1 was immunoprecipitated for determining the level of phosphorylation. **C**, PI3K -mediated AKT phosphorylation. COS7 cells were transfected with myc-PI3K p110 and p101 together with FLAG-G 3 2 or FLAG-G 3s 2 as indicated. 24 hr post-transfection, phosphorylation of endogenous AKT was determined. **D**, PLEKHG2 activation. HEK293 cells were co-transfected with expression vectors for SRE-luciferase, EGFP, PLEKHG2, and different concentration of FLAG-G 3 2 or FLAG-G 3s 2 as indicated. 24 hr post-transfection, luciferase activities were measured. After normalization with the level of GFP expression, relative luciferase activities are shown. Displayed are representative images and quantitative data from three to four experiments expressed as the mean ± S.E. \* p<0.05 indicate significance.

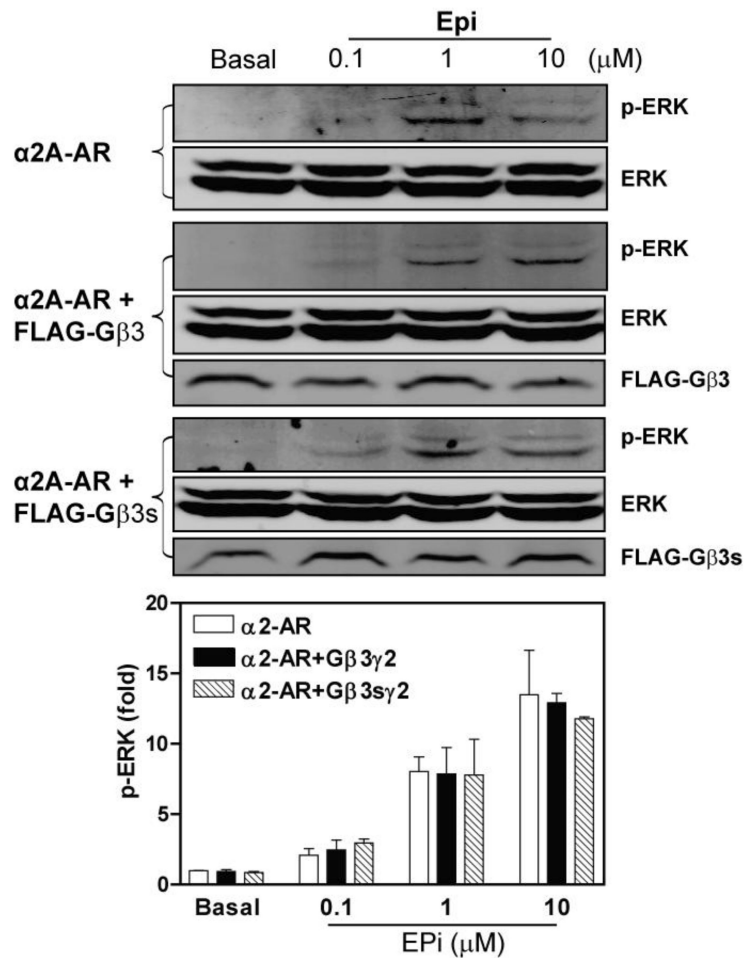


**Figure 6. Overexpression of G<sub>3</sub> or G<sub>3s</sub> does not alter GPCR signaling**

HEK293 cells were transfected with FLAG-G<sub>3</sub> or FLAG-G<sub>3s</sub> together with G<sub>2</sub> and α2A-AR. After serum-starvation overnight, cells were stimulated with epinephrine (Epi) at the indicated concentration for 5 min and then processed for Western blotting. Displayed are representative images and quantitative data from three separate experiments expressed as the mean ± S.E.

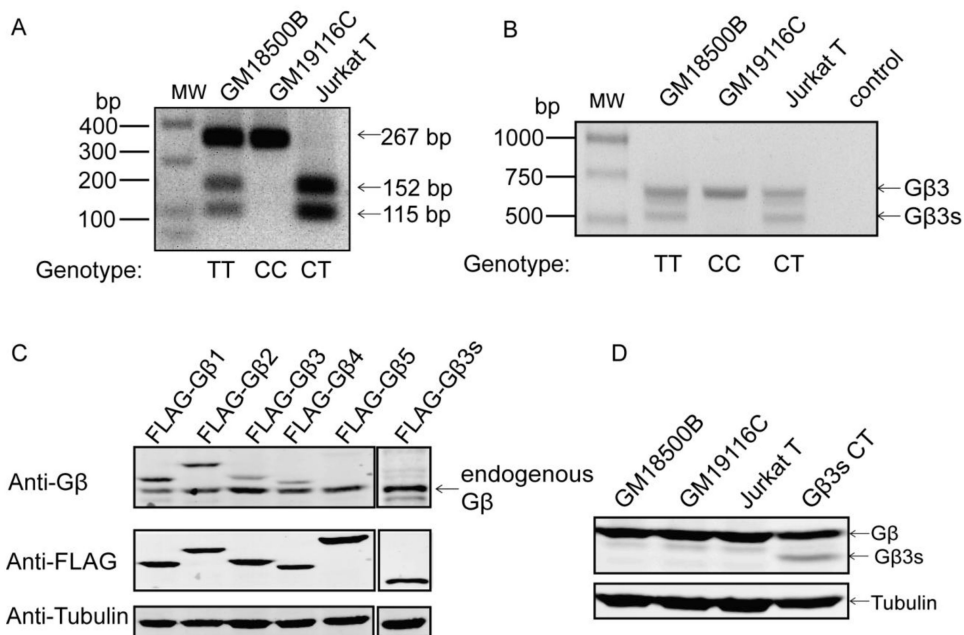


**Figure 7. Genotypes of G<sub>3</sub> C285T polymorphism and detection of G<sub>3</sub>- and G<sub>3s</sub>-specific transcripts and G<sub>3s</sub> protein in human lymphocytic cell lines**

*A*, genomic DNA was extracted from lymphocytic cell lines. A combination of PCR and digestion of the PCR product with the restriction enzyme BseDI was used for genotyping, and the results are indicated underneath the gel image. CC, C825C homozygous; TT, C825T homozygous; CT, C825T heterozygous. *B*, RT-PCR was performed to identify G<sub>3</sub>- and G<sub>3s</sub>-specific transcripts (651bp and 528 bp, respectively) in lymphocytic cell lines. Control was performed in the absence of the template. *C*, the ability of the pan anti-G<sub>3</sub> antibody to detect multiple FLAG-tagged G<sub>3</sub> isoforms expressed in HEK293 cells. *D*, detection of G<sub>3s</sub> protein in lymphocytic cell lines with a pan anti-G<sub>3</sub> antibody. Lysates from HEK293 cells expressing untagged G<sub>3s</sub> were used as control (G<sub>3s</sub> CT). The bands correspond to endogenous G<sub>3</sub> and overexpressed G<sub>3s</sub> are indicated. Displayed are representative images of at least three separate experiments.

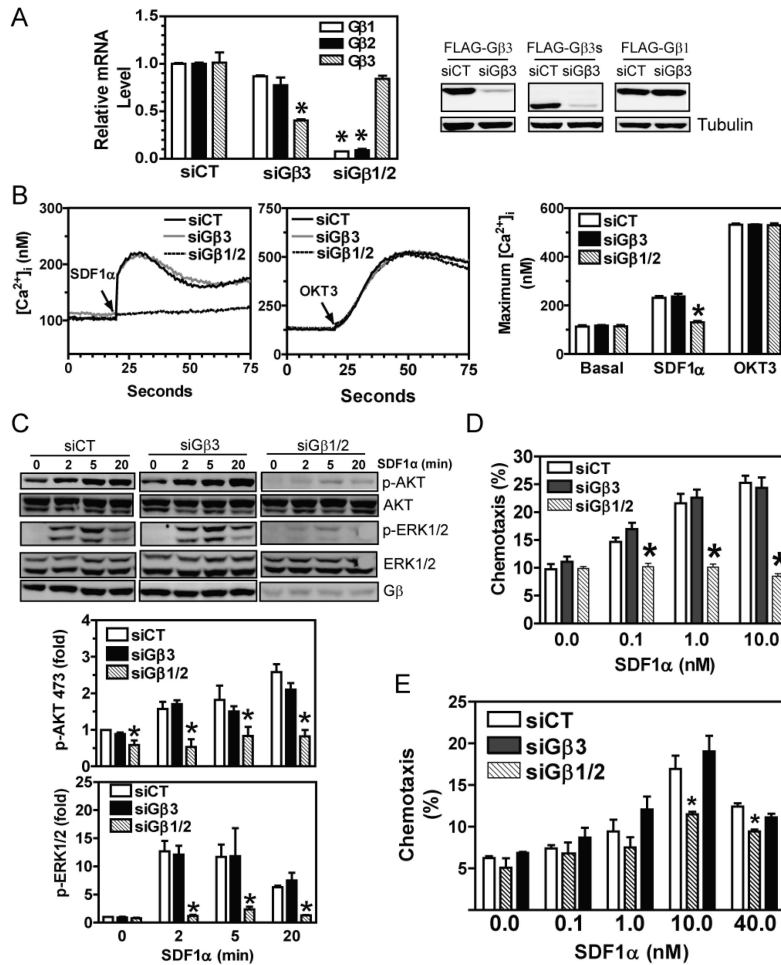


**Figure 8. G 3 and G 3s are not required for SDF1 -stimulated signaling and chemotaxis**  
**A**, Jurkat T cells were transiently transfected with a control siRNA (CT) or siRNAs against G 3/G 3s (siG 3) or G 1/G 2 (siG 1/2) and processed for determining the effects on the level of G 3, G 1 and G 2 mRNAs by qRT-PCR (left panel), and co-expressed Flag-G 3 and G 1 protein by Western blotting (right panel). **B-D**, effects of inhibiting G 3, G 1 and G 2 in Jurkat T cells on SDF1 (100 nM) or OKT3 (5  $\mu$ g/ml)-stimulated Ca<sup>2+</sup> signaling (B) and the phosphorylation of AKT and ERK1/2 (C), and SDF1 -stimulated chemotaxis (D). Displayed are representative images and quantitative data from at least three independent experiments expressed as the mean  $\pm$  S.E. \**p*<0.05 *versus* siCT **E**, effect of inhibiting G 3, G 1 and G 2 on SDF1 -induced chemotaxis of GM19116C cells. \**p*<0.05 indicates significance *versus* siCT.